

DEVELOPMENT AND EVALUATION OF A MODEL FOR FIRE-RELATED HSC SPALLING FAILURE

○T.Tanibe (Taiheiyo Material) M.Ozawa(Gunma University) R.Kamata(Taiheiyo Material) Y.Uchida(Gifu University)
K.Rokugo(Gifu University)

Contact : Mitsuo Ozawa Dr.(Eng), Associate Professor, ozawa@gunma-u.ac.jp

Gunma University, Department of Civil Engineering, Concrete Engineering Laboratory, 1-5-1, Tenjin-cho, Kiryu, Gunma, Japan 376-8515

Abstract : This paper reports on an experimental study regarding the behavior of restrained high-strength concrete in response to the type of extreme heating associated with fire. The study was intended to support estimation of thermal stress from the strain in a restraining steel ring and vapor pressure in restrained concrete under the conditions of a RABT 30 rapid heating curve. Thermal stress calculation was based on the thin-walled cylinder model theory. A spalling failure model based on a strain failure model was also proposed. The results indicated that such modeling enables estimation of the point at which spalling starts during heating and the consequent spalling depth.

1. Introduction

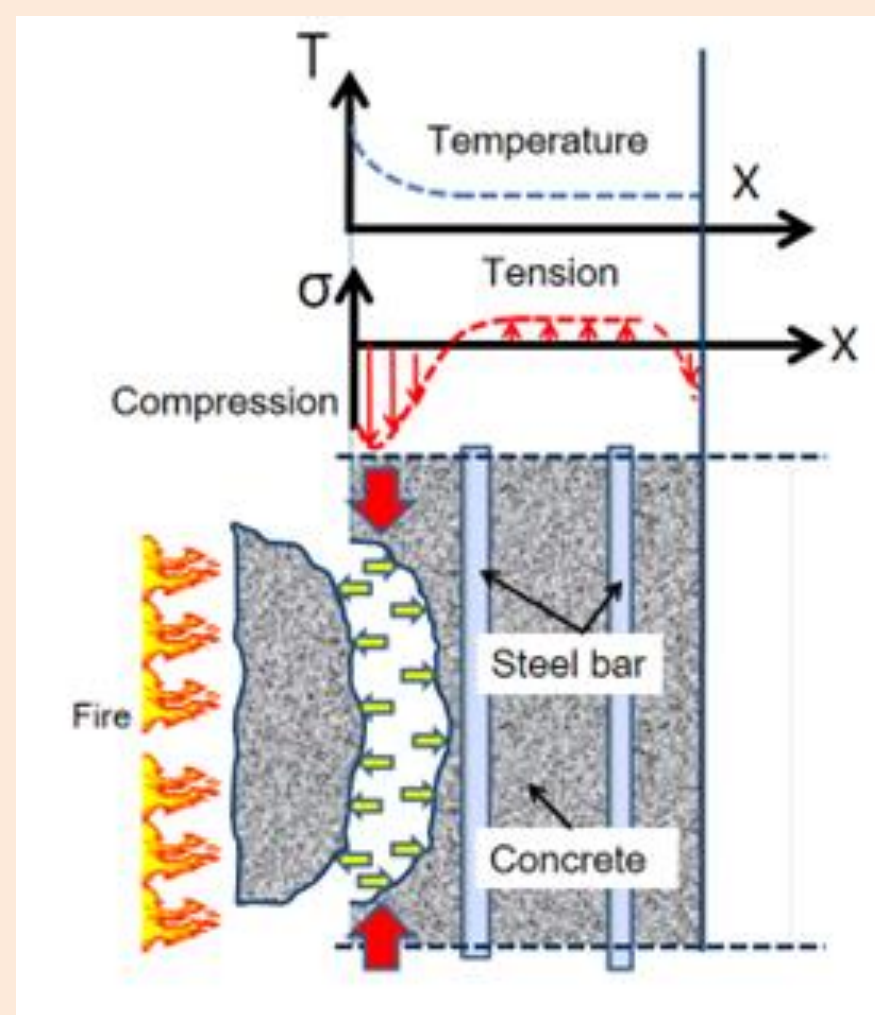


Fig.1 Thermal stress

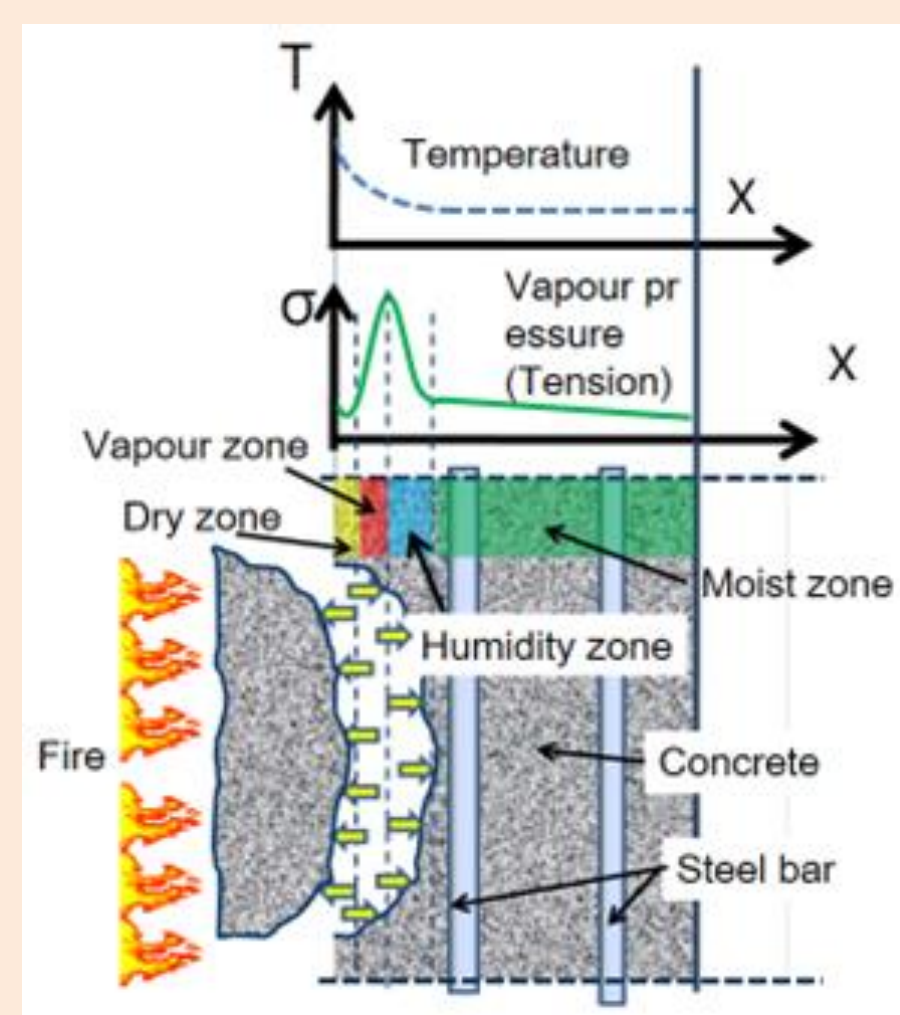


Fig.2 Vapor pressure

Fire poses one of the most serious risks to concrete buildings and structures because it often results in explosive spalling of concrete. There are two mechanisms by which concrete can be damaged by fire. The first is restrained thermal dilation resulting in biaxial compressive stress states parallel to the heated surface, which leads to tensile stress in the perpendicular direction (Fig.1).

The second is the build-up of concrete pore pressure due to vaporization of physically/chemically bound water resulting in tensile loading on the microstructure of the heated concrete (Fig.2).

However, few reports to date have outlined actual experimental studies on the exact influence of thermal stress. The authors previously reported that a method involving the restraint of concrete with steel rings in heat testing can be used to clarify characteristics of thermal stress and explosive spalling behavior.

2. Model for Estimation of Thermal Stress and Strain Failure

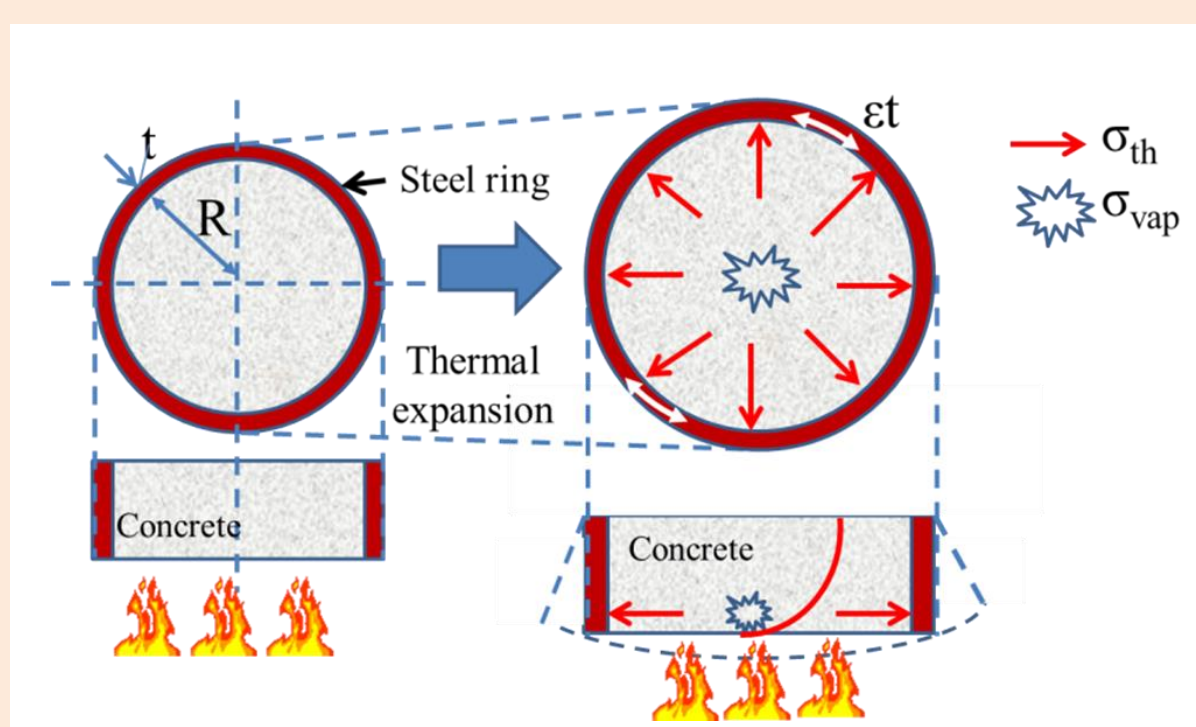


Fig.3 Estimation of thermal stress

Figure 3 shows the method used to estimate thermal stress. Thermal stress calculation was based on the thin-walled cylinder model theory as shown by Eqs. (1) and (2).

$$\sigma_{re} = \sigma_{th} + \sigma_{vap} \quad (1)$$

$$\sigma_{re} = \varepsilon_t \cdot E_s \cdot \frac{t}{R} \quad (2)$$

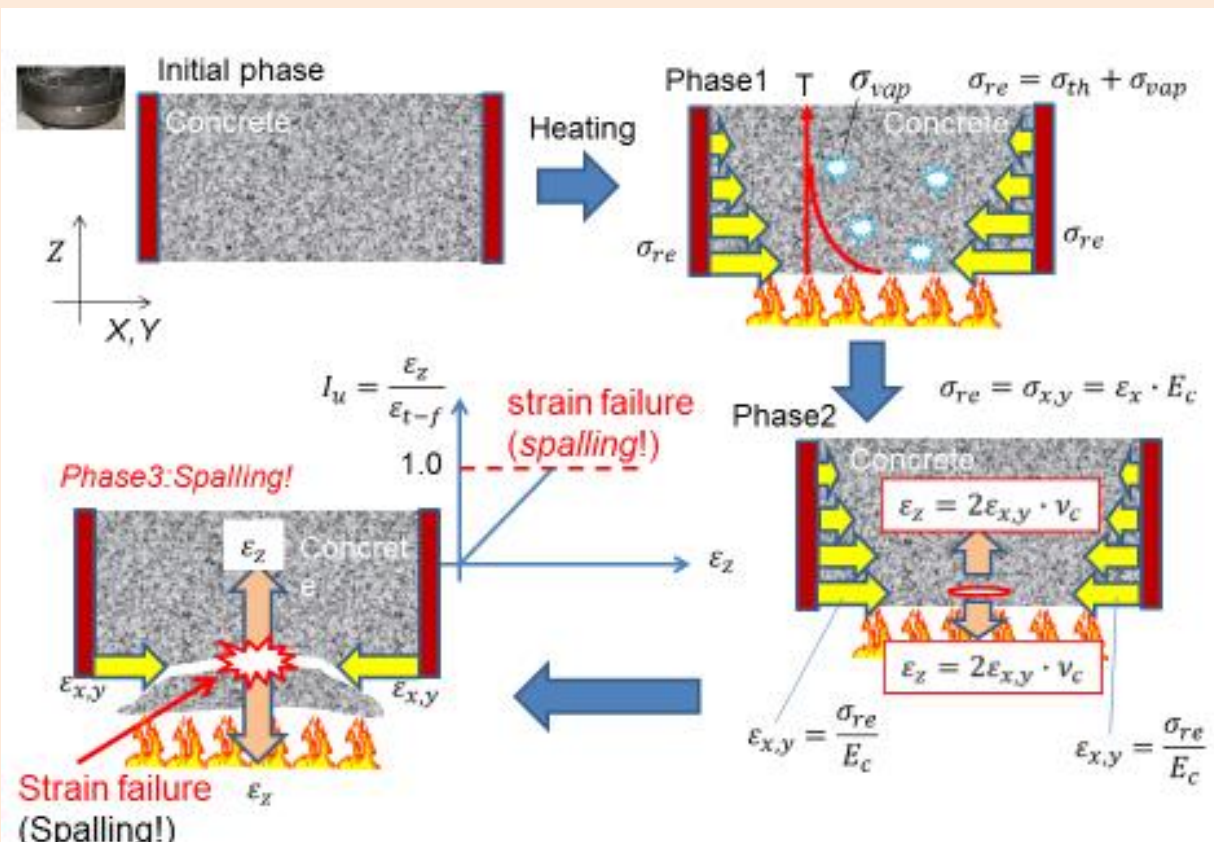


Fig.4 Strain failure model of explosive spalling

Figure 4 shows a strain failure model of explosive spalling under thermal stress. Strain at a certain depth from the heated surface was calculated using eqs. (3) and (4), and the index of the strain failure model was given by Eq. (5).

Tensile strain failure occurred when the index of the strain failure model exceeded 1.0 ($I_u > 1.0$).

$$\sigma_{re} = \sigma_{x,y} = \varepsilon_{x,y} \cdot E_c \quad (3)$$

$$\varepsilon_z = 2\varepsilon_{x,y} \cdot \nu_c \quad (4)$$

$$I_u = \varepsilon_z / \varepsilon_{t-f} \quad (5)$$

3. Outline of Experiment

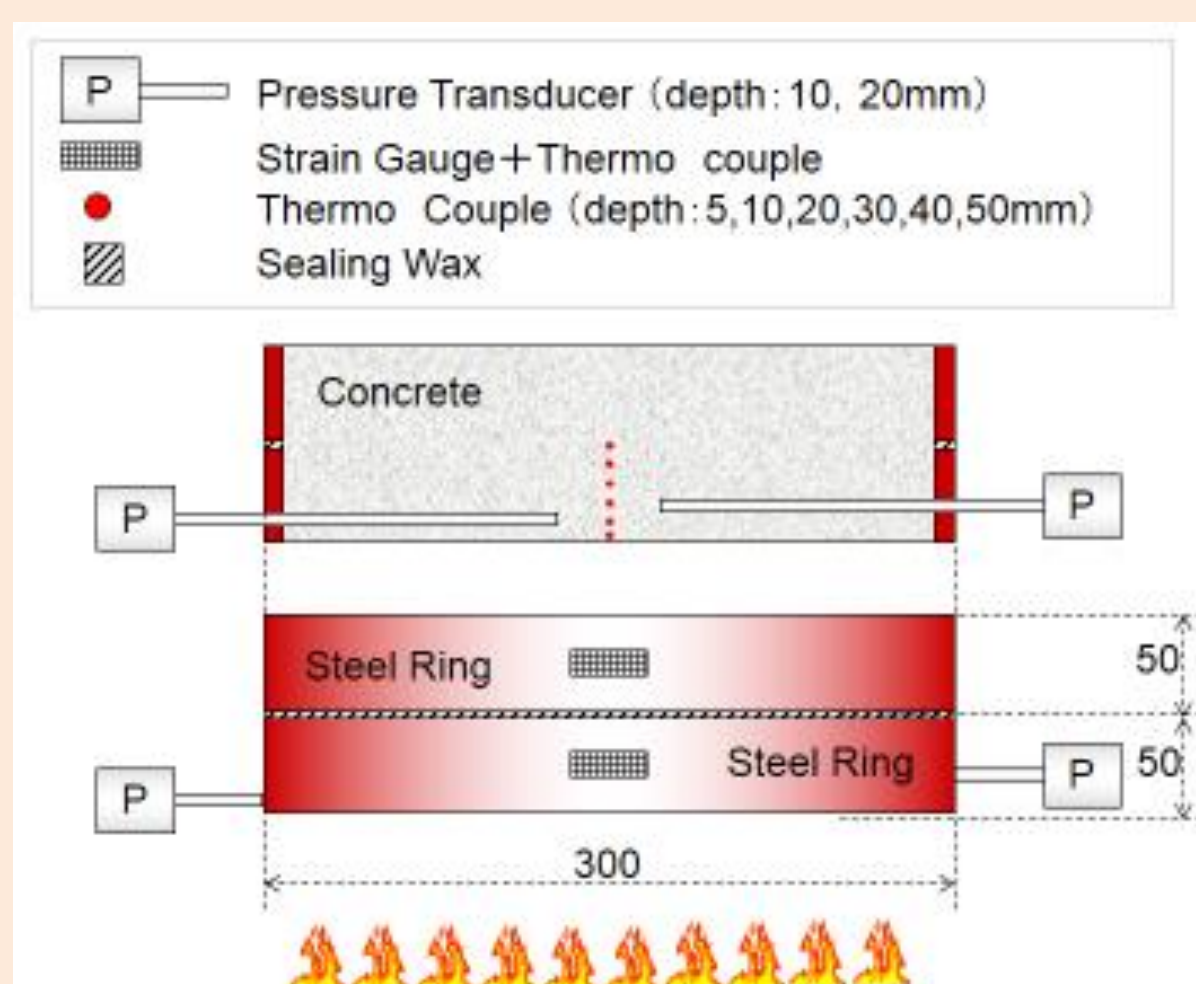


Fig. 5 Specimen

Figure 5 shows the configuration and dimensions of the two specimens used with two pairs of steel rings (diameter: 300 mm; thickness: 8 mm; length: 50 mm).

Two strain gauges and two thermocouples were attached at 25 and 75 mm from the heated surface and outer surface of the steel rings.

Stainless steel pipes (inner diameter: 2 mm; length: 200 mm) were placed in the concrete at distances of 10 and 20 mm from the heated surface and parallel to it.

Six type-K thermocouples were placed in the central zone of the specimens at 5, 10, 20, 30, 40 and 50 mm from the heated surface.

The heating tests were based on a RABT 30 heating curve.

4. Results and Discussion

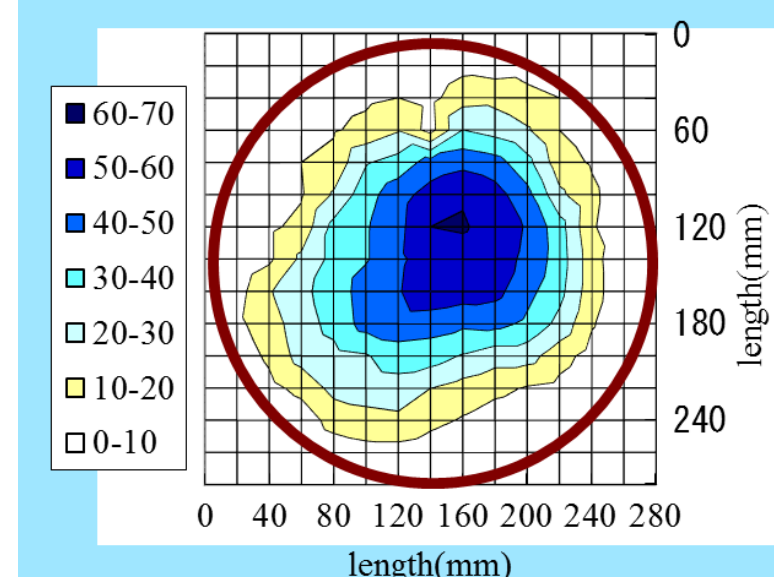


Fig.6 Spalling depth

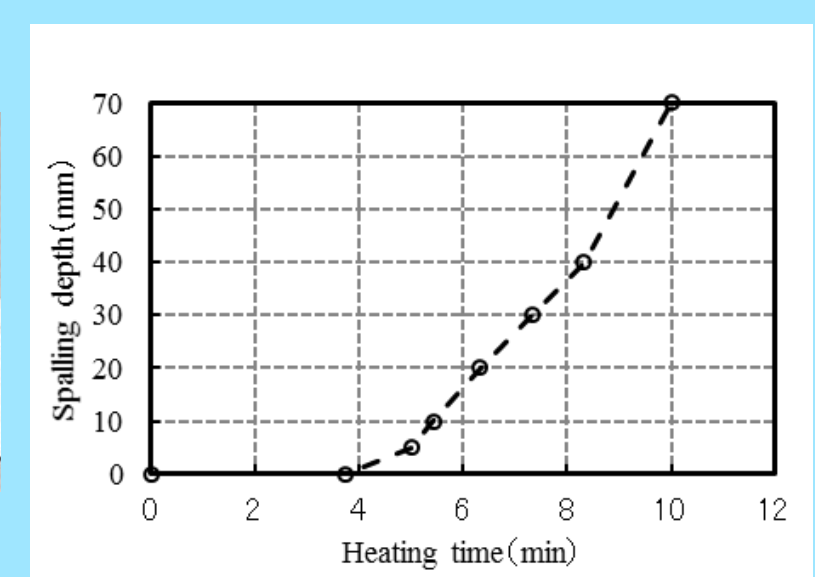


Fig.7 Spalling depth and time

Figure 6 shows results for the depth of spalling after the heating test. The maximum value was about 70 mm, and the depth at the center part was greater than that at the outer part. The specimens were severely damaged.

Figure 7 shows the relationship between spalling depth and time during the heating test. Spalling began approximately 4 minutes after heating was started, and the spalling rate was about 10 mm/min.

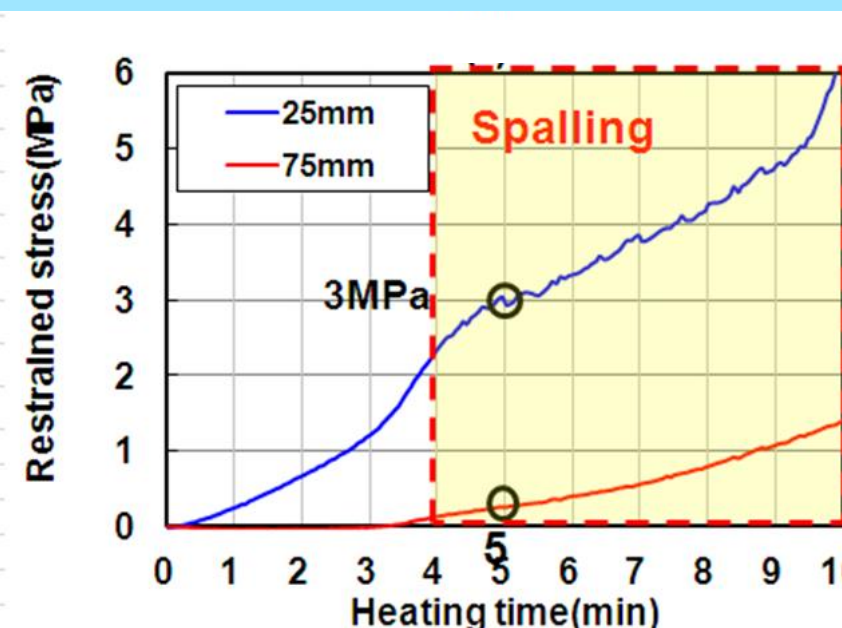


Fig.8 Restrained stress

Figure 8 shows the results of restrained stress calculation based on ring strain at a point 25 mm from the heated surface. After 5 minutes of heating, the value reached 3 MPa at this point.

$$\sigma_{x,y}(z) = \sigma_{x,y-25} \cdot \frac{\Delta T_c(z)}{\Delta T_{c-25}} \quad (6)$$

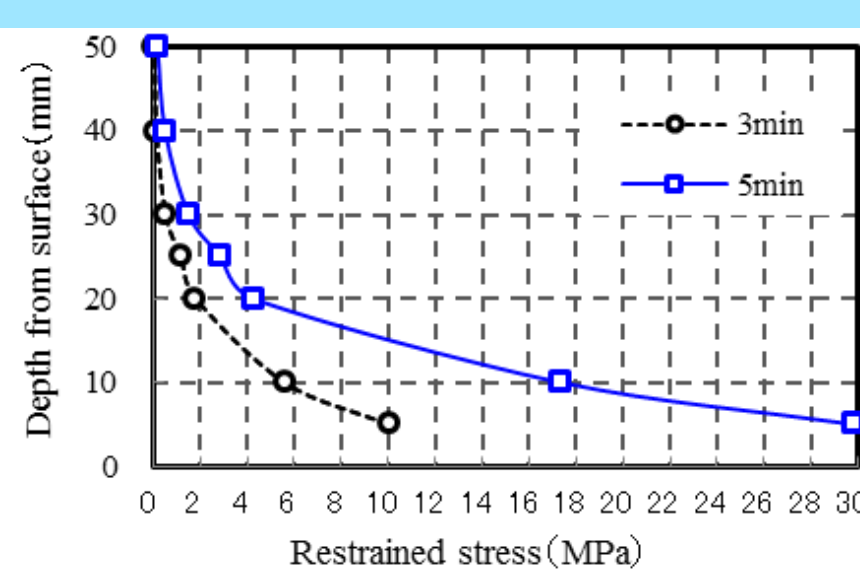


Fig.9 for distribution of restrained stress at three and five minutes

Distribution of restrained stress was estimated using Eq. (6). Restrained stress itself was calculated using an experimental value at a point 25 mm from the heated surface, and was assumed to be in proportion to the temperature increment.

Figure 9 shows the results for distribution of restrained stress at 5 and 5 minutes.

After 5 minutes of heating, restrained stress 5 mm from the heated surface was about 30 MPa.

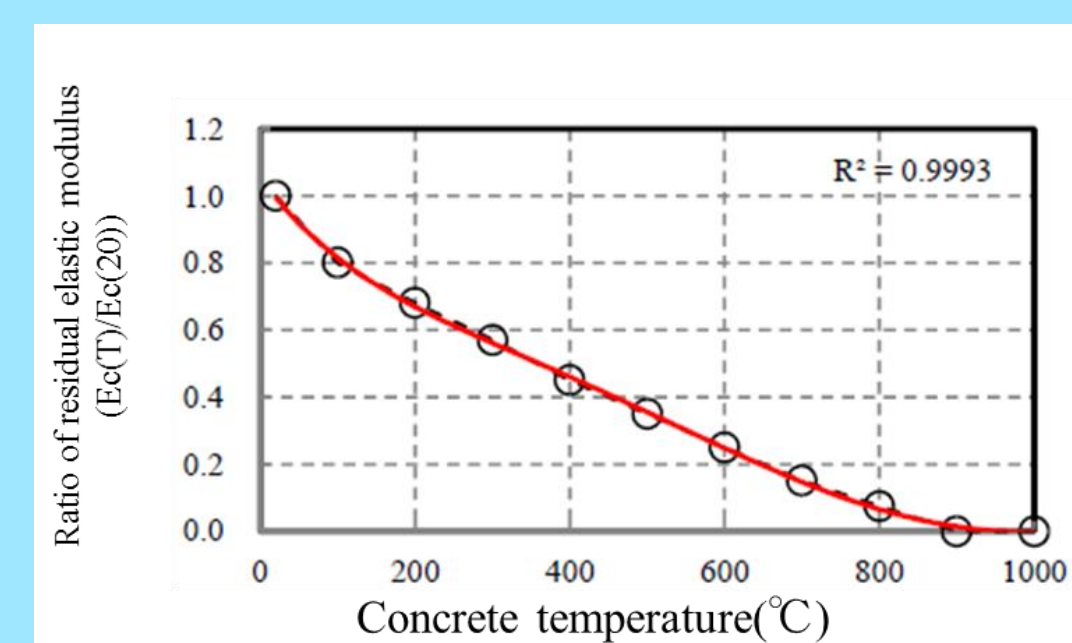


Fig.10 Ratio of residual elastic modulus and temperature

In this work, a strain failure model of explosive spalling was verified. The relationship between the ratio of residual elastic modulus and temperature was used in the AIJ model as shown in Fig. 10.

The residual Poisson's ratio of concrete upon heating was 0.2 and the ultimate strain upon tensile failure ranged from 200 to 500 μ . The spalling depth was estimated using eqs. (3) to (6).

It was assumed that spalling occurred if the index of the strain failure model in Eq. (6) exceeded 1.0. Figure 14 shows spalling depth comparison with experimental and estimation values.

It can be seen that the maximum spalling depth was estimated to be about 40 mm at nine minutes. These outcomes clearly indicate that the proposed model can be used to estimate spalling depth up to 9 minutes from the start of heating.

In this study, the range from 200 to 500 μ for the ultimate strain upon tensile failure had no influence on spalling depth estimation.

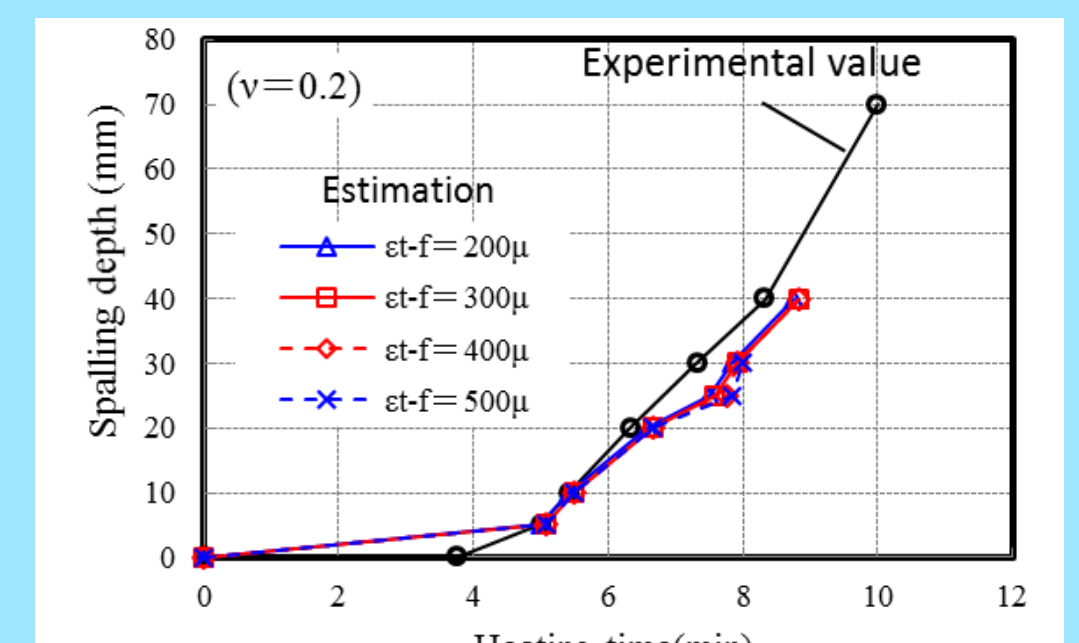


Fig.11 Spalling depth (Experiment vs. Estimation)

5. Conclusion

The results obtained from the study can be summarized as follows:

1. The proposed method involving the restraint of concrete with steel rings in heat testing can be used to clarify characteristics of thermal stress and explosive spalling behavior.
2. The proposed spalling failure model based on a strain failure model was found to support estimation of spalling depth up to nine minutes from the start of heating.

Acknowledgement

This study was supported by a Grant-in-Aid for Scientific Research C (General) from the Japan Society for the Promotion of Science 2013 No. 25420459 (Head: Dr. M. Ozawa) and Japan's Kajima Foundation 2013. The authors would like to express their gratitude to the organization for its financial support.

THERMAL PROPERTIES OF JUTE FIBER CONCRETE AT HIGH TEMPERATURES

○Mitsuo Ozawa(Gunma University, JPN) , Choe G. Cheol(Chung-nam National University, KOREA),
Kim G. Yong(Chung-nam National University, KOREA) , Ryoichi Sato(Gifu University, JPN), Keitetsu Rokugo(Gifu University, JPN)

Contact : Mitsuo Ozawa Dr.(Eng), Associate Professor, ozawa@gunma-u.ac.jp
Gunma University, Department of Civil Engineering, Concrete Engineering Laboratory,1-5-1, Tenjin-cho, Kiryu, Gunma, Japan 376-8515

Abstract : In this study, the effects of high temperatures on the compressive strength and elastic modulus of HPC with **pp and jute fiber (jute fiber addition ratio: 0.075 vol%; length: 12 mm; PP fiber addition ratio: 0.075 vol%; length: 12 mm)** were experimentally investigated. The work was intended to clarify the influence of elevated temperatures ranging from 20 to 500°C on the material mechanical properties of HPC at 80 MPa.

1. Introduction

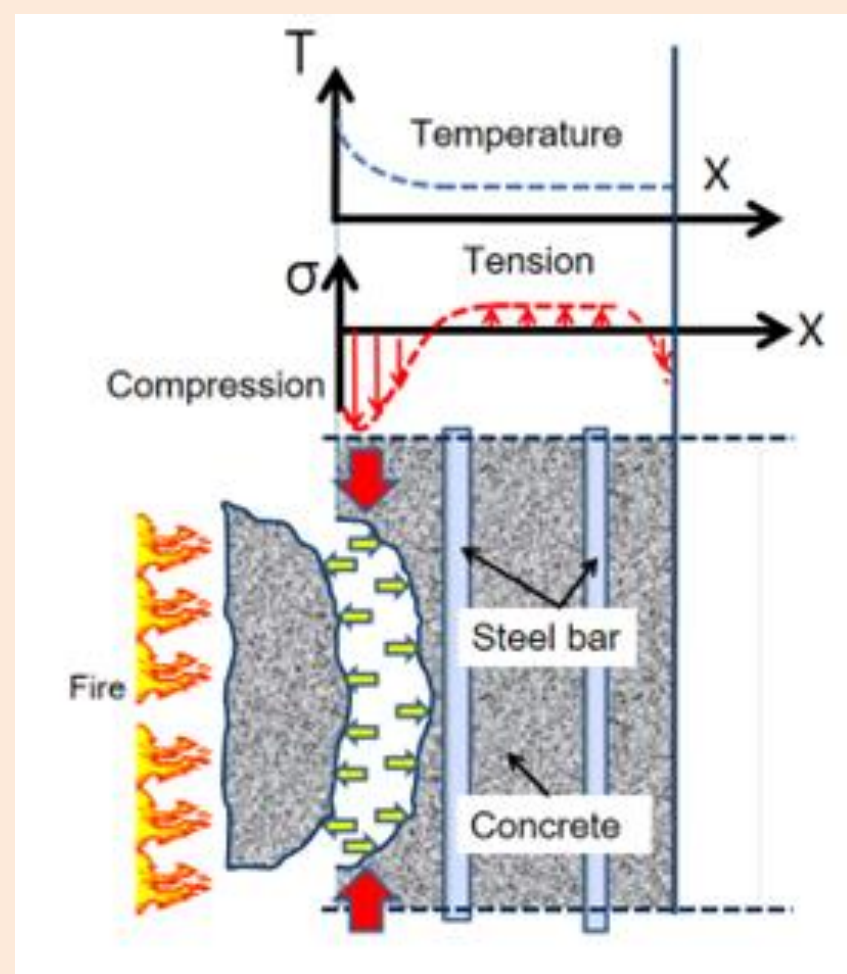


Fig.1 Thermal stress

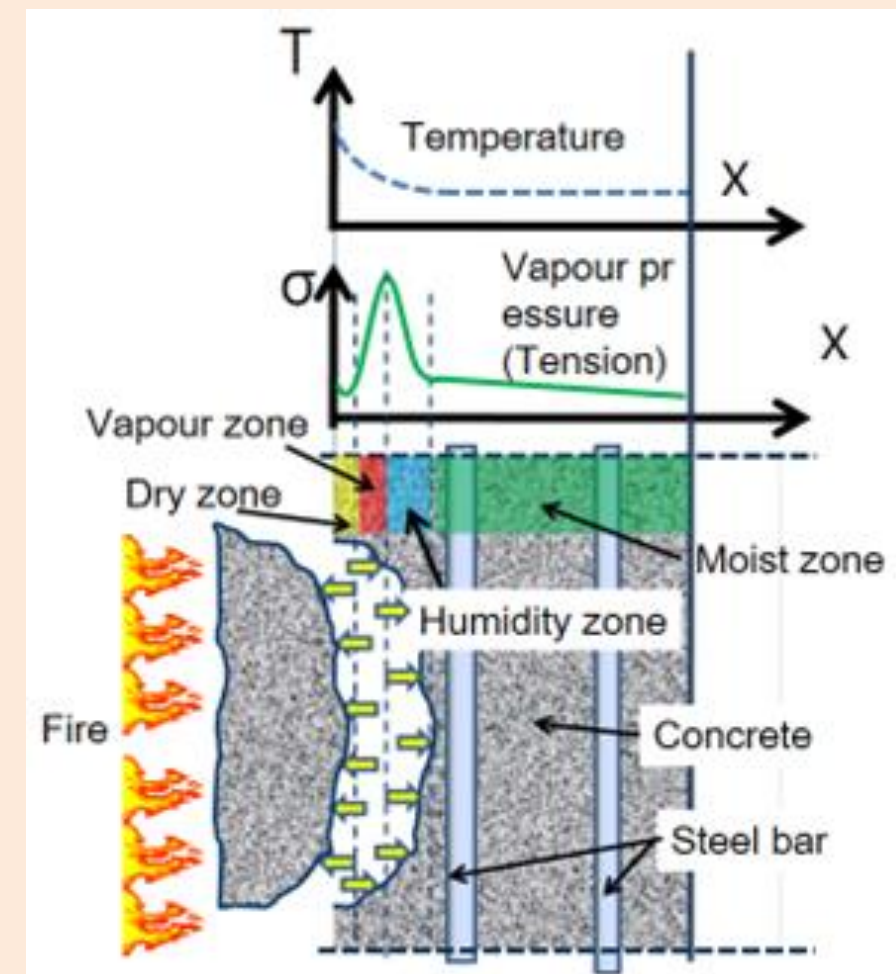


Fig.2 Vapor pressure

The behavior of high-performance concrete (HPC) at high temperatures is very complex, and also affects the global behavior of heated HPC-based structures. Concrete exposed to fire undergoes spalling owing to two phenomena. The first is restrained thermal dilation resulting in biaxial **compressive stress** states parallel to the heated surface, which leads to tensile stress in the perpendicular direction (Fig.1).

The second is the build-up of concrete **poressure** due to vaporization of physically/chemically bound water resulting in tensile loading on the microstructure of the heated concrete (Fig.2).

Researchers have also reported how various types of fiber affected the mechanical properties of cement-based materials at high temperatures. Adding synthetic fiber (especially the polypropylene (PP) type) to HPC is a widely used and effective method of preventing explosive spalling.

Although researchers have experimentally determined the permeability of heated PP-fiber-reinforced HPC, few studies have investigated how adding natural fiber such as jute to this type of concrete might prevent spalling.

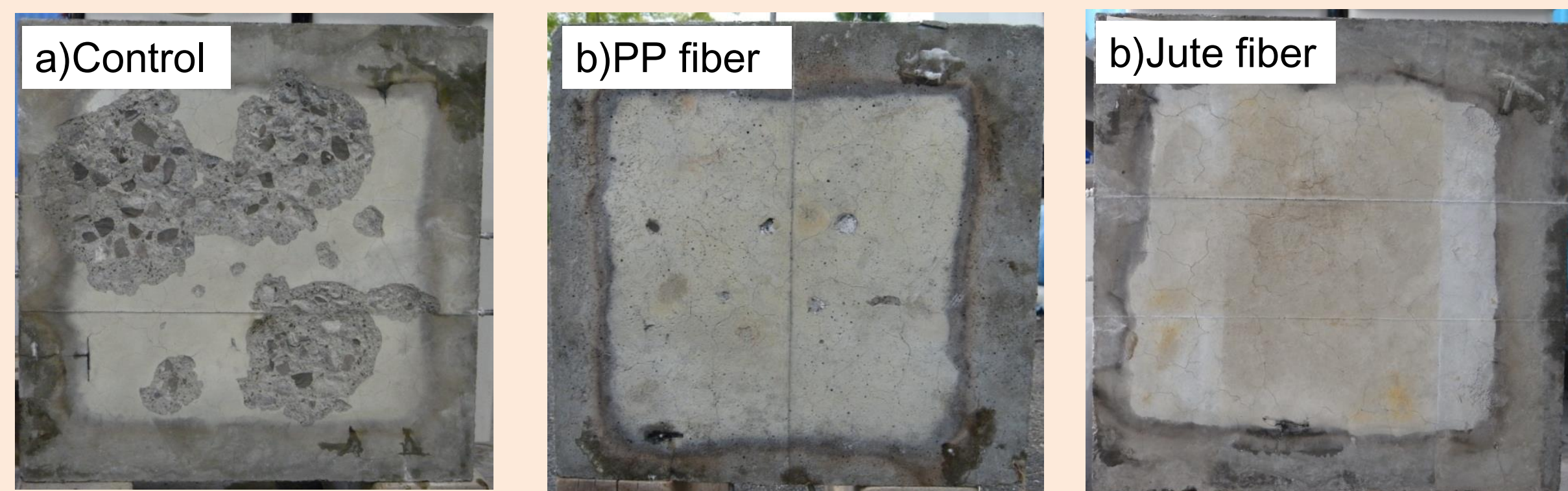


Photo.1 Heating test results(RABT30)

Photo 1 shows images of the specimens after the heat tests. The control specimen showed severe damage and had a maximum spalling depth of 7 mm. However, the jute, WSPVA, and PP specimens did not undergo explosive spalling in recent research.

2. Experimental program

Table 1 Experimental program

W/C	Fiber	Fiber contents (vol.%)	Heat	Test item
0.3	Jute	0	1°C/min	<ul style="list-style-type: none"> Strength properties - Compressive strength (MPa) - Elastic modulus (GPa)
	Polypropylene	0.075		<ul style="list-style-type: none"> Residual strength properties - Compressive strength (MPa) - Elastic modulus (GPa) Thermal strain

The experimental program is summarized in Table 1. To investigate the effects of jute and pp fiber amounts and the residual mechanical properties (compressive strength, elastic modulus, thermal strain) of concrete exposed to high temperatures, the water-to-cement (w/c) ratio adopted was 0.30, and 0, 0.075% of jute and PP fiber by concrete volume were used.



Figure 3 Jute in concrete(SEM)

Figure 3 shows the jute, whose fiber had a straw-like structure as highlighted by scanning electron microscopy (SEM).

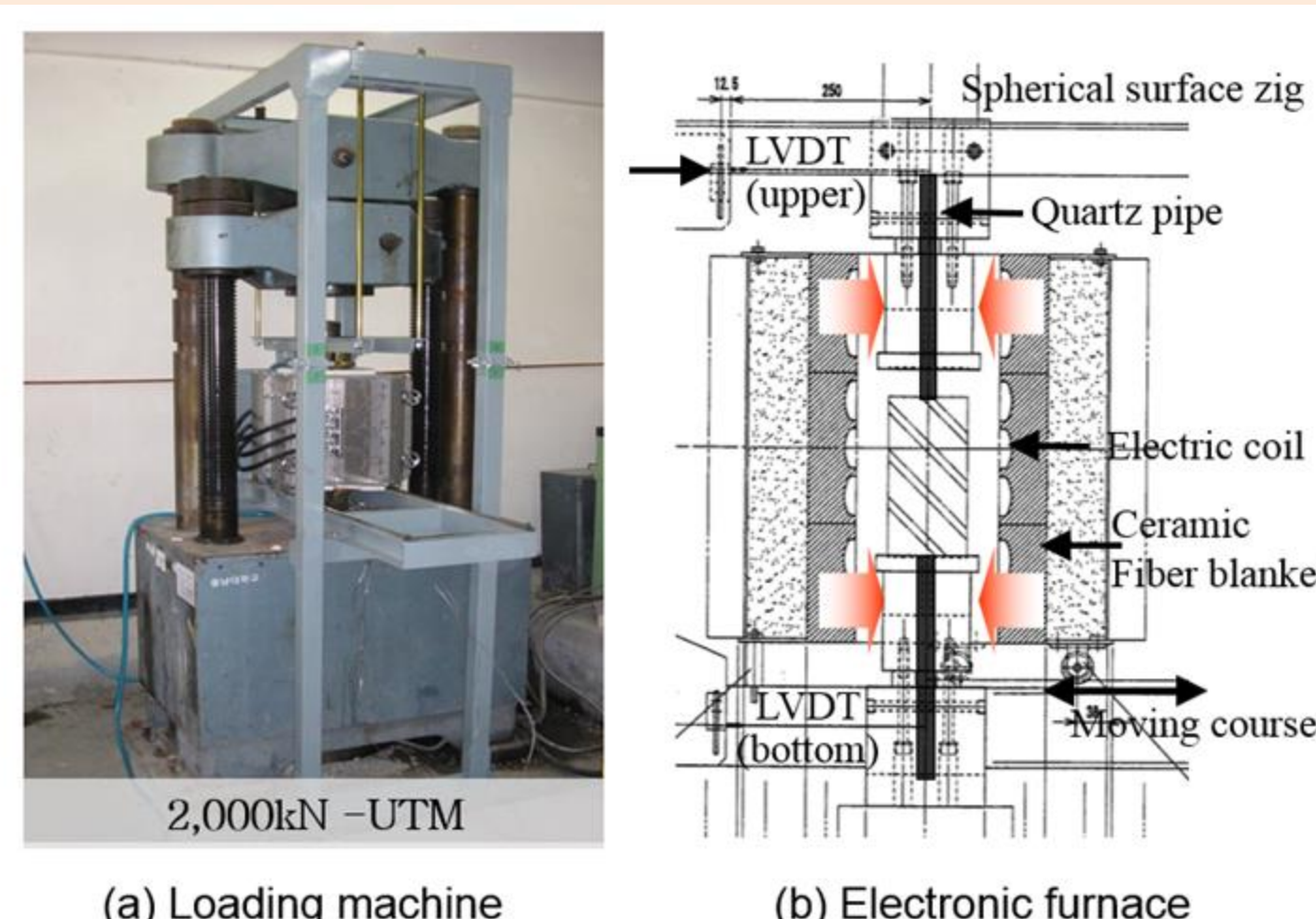


Figure 4 Test setup

The tests were performed in a closed-loop servo-controlled 4,600-kN hydraulic testing machine equipped with an electric furnace as shown in Fig. 4.

3. Temperature control

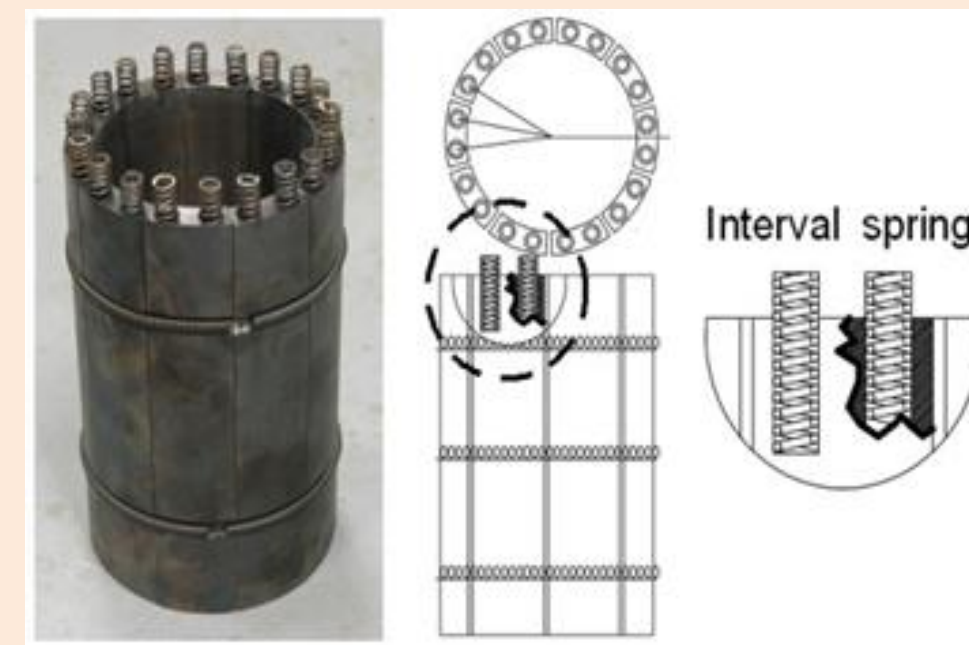


Figure 5 Heating attachments

Special cylindrical carbon-based alloy attachments were designed to transmit loading from the frame to the specimen under high-temperature conditions, and a continuous circulation water-cooling system was used to protect the instruments and avoid heating the testing frame.

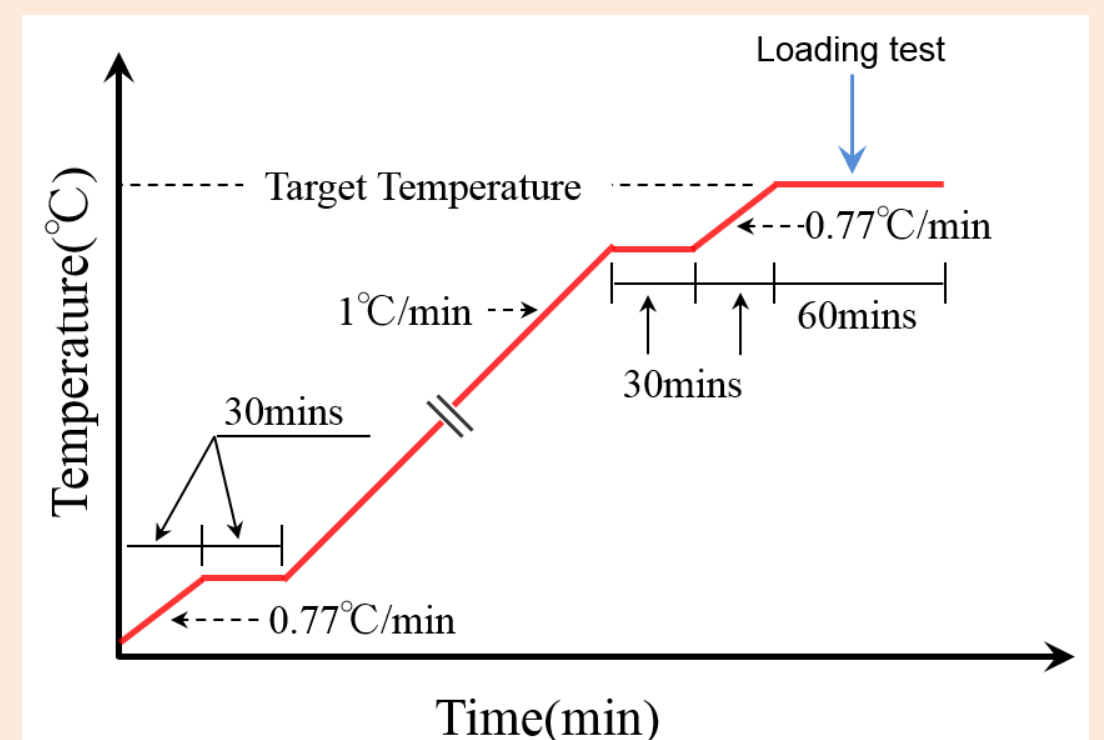


Figure 6 Heating rate

For each set of tests at a given temperature, three specimens from the same batch were also tested at room temperature.

The target temperatures were varied from 100 to 500°C at 100°C increments. As shown in Fig. 5, the rate of heating for all specimens was set at 1.0°C/min using a RILEM TC 129-MHT unit.

4. Results and Discussion

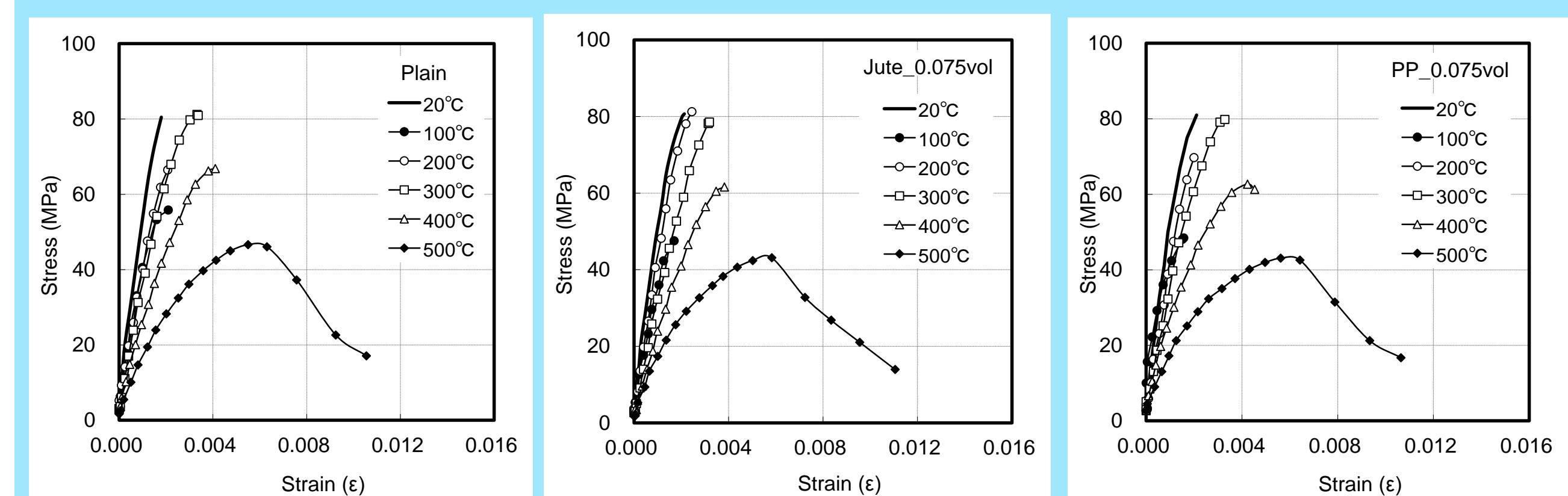


Fig.6 Stress-strain curve

For temperatures of 300°C or below, the curve shape essentially exhibits no change from that of unheated concrete. After exposure to 500°C, specimen heat damage increases gradually and the stress-strain curve flattens as the temperature rises.

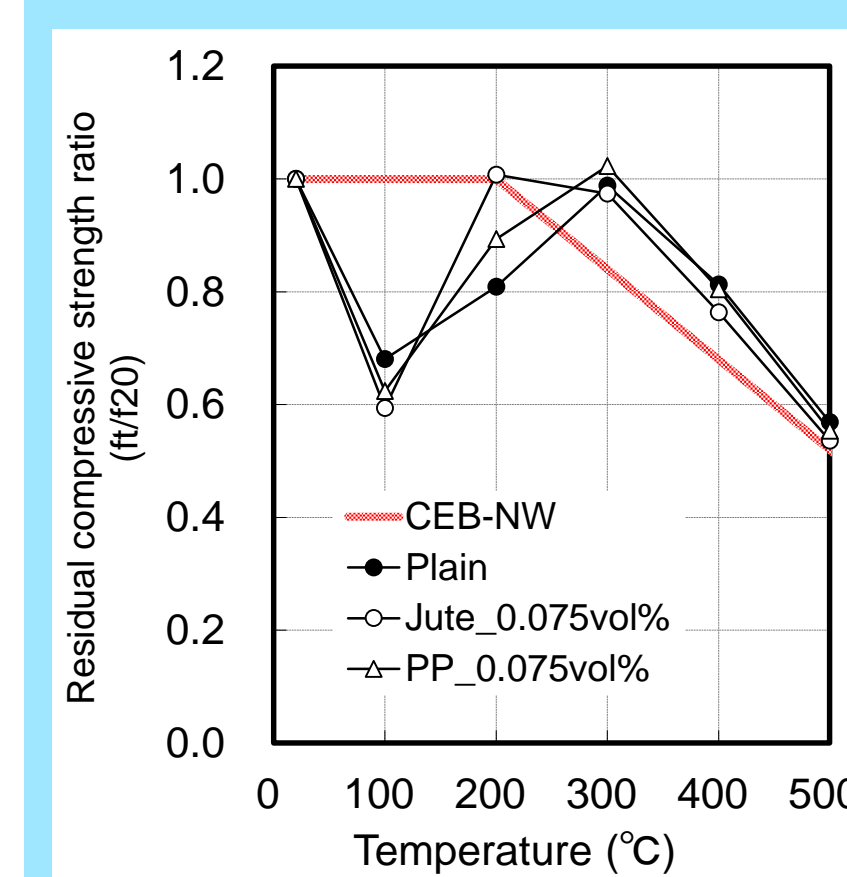


Fig.9 Residual compressive strength ratio

Initially, as the temperature increased to 100°C, strength decreased in relation to that observed at room temperature. Strength at 100°C was about 60% of the room-temperature value.

With further increases in temperature at 200°C, the specimens recovered strength to 100% of the room-temperature value.

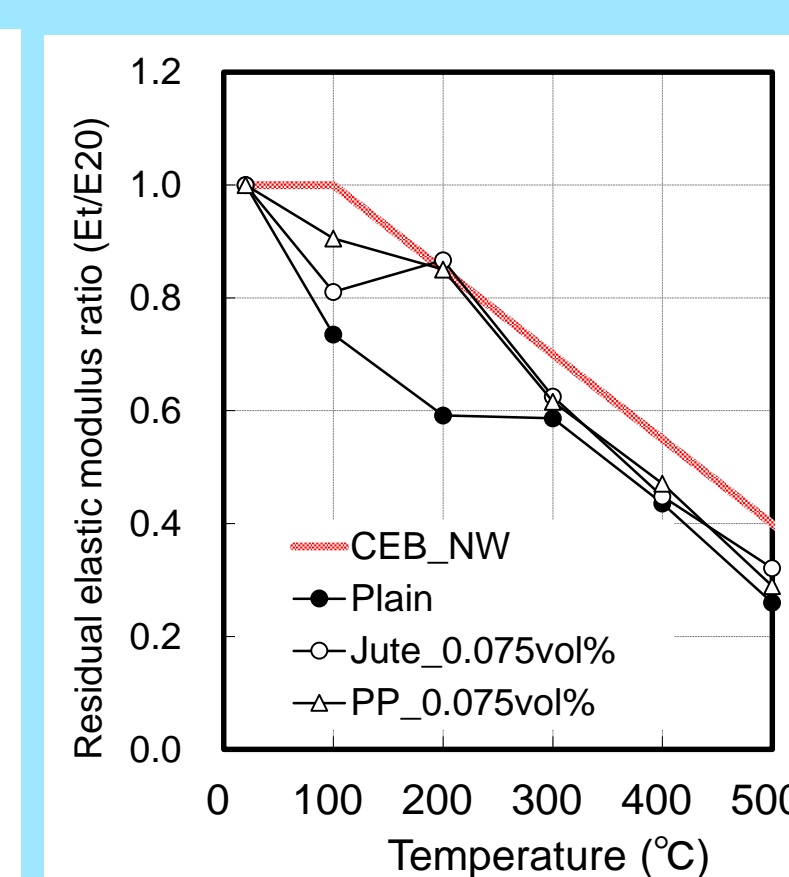


Fig.10 Residual elastic modulus ratio

As the temperature increased to 100°C, the elastic modulus decreased in relation to that observed at room temperature. The elastic modulus at 100°C was 70–90% of the room-temperature value.

With further increases in temperature, the specimens recovered elastic modulus to 90% of the room-temperature values for jute-fiber and pp-fiber concrete.

Up to around 300°C, the elastic modulus of all three types of high-strength concrete decreased in a similar fashion, reaching about 60% of their respective initial values.

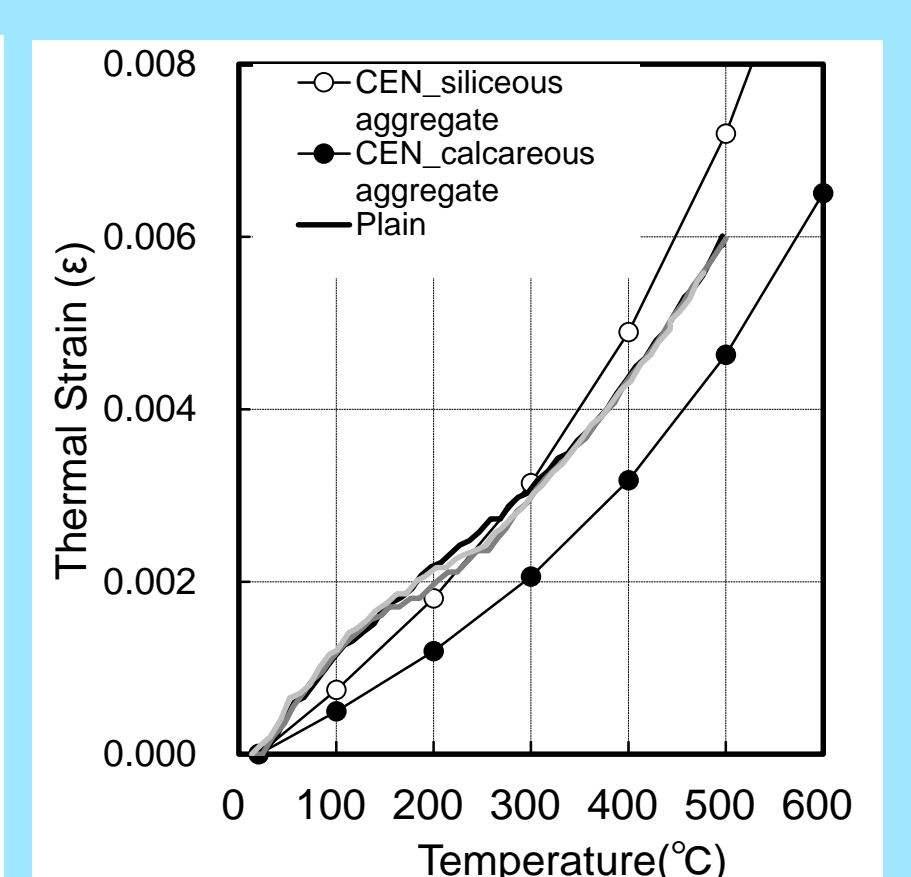


Fig.11 Thermal expansion strain

Thermal expansion in all specimens increased between 20 and 500°C, and thermal expansion strain in all specimens was 0.006 at 500°C.

This was considered mainly due to thermal expansion of the concrete's constituent aggregates.

5. Conclusion

The above results can be summarized as follows:

- HSC with jute fiber showed a compressive strength loss of about 40% at 100°C before recovering to full strength between 200 and 300°C.
- The elastic modulus of high-strength concrete decreased by 10–40% between 100 and 300°C. At 500°C, the elastic modulus was only 30% of the room-temperature value.
- The thermal expansion strain of all specimens was 0.006 at 500°C.